Coupled Burgers equations: A model of polydispersive sedimentation

Sergei E. Esipov
James Franck Institute and Department of Physics, University of Chicago, 5640 South Ellis Avenue, Chicago, Illinois 60637
(Received 27 December 1994; revised manuscript received 13 April 1995)

This paper compares theory and experiment for the kinetics of time-dependent sedimentation. We discuss noninteracting (apart from hydrodynamic interaction) suspensions and colloids which may exhibit behavior similar to the one-dimensional motion of compressible gas. The velocity of sedimentation (or creaming) depends upon the volume fraction of the constituting particles and leads to Burgers-like equations for concentration profiles. It is shown that even the bidispersive system of two coupled Burgers equations has rich dynamics. The study of a polydispersive case reveals a continuous "renormalization" of the polydispersity. We compare the Burgers system evolution with the experimental results on monodispersive and polydispersive sedimentation.

PACS number(s): 05.60.+w, 05.40.+j, 47.55.Kf

I. INTRODUCTION

The study of the motion of particles in a fluid goes back to Einstein and before that to Brown. Here we consider the effect of gravity upon the particles. If they are heavier than the surrounding fluid the resulting motion is called sedimentation; if lighter it is creaming. The conventional and simplest problem involves the evolution of an initially uniform suspension or colloid. At the bottom (of the test tube) there appears the sediment, and at the top water free of particles which is called the supernatant. Between these regions there is the original suspension itself. Thus two interfaces are created, and they spread and propagate towards each other. The description of the bottom interface invokes high volume ratios leading to "trafficlike" problems with possible jams and other instabilities whereby additional interfaces may emerge [1]. In this paper we address the evolution of the top interface in the dilute limit, in which the volume fraction of the particles is much less than 1. We apply the continuity equation which describes the conservation of species with concentration $c(x,t)$ and current $\mathbf{J}(x,t)$. In the case of very small particles which experience Brownian motion this equation reads ([2], §58,59)

$$\partial_t c + \mathrm{div}\mathbf{J} = 0 \ . \tag{1.1}$$

The particle flux $\mathbf{J}$ is produced by external forces (such as gravity), and also depends on gradients of concentration, pressure, and temperature. In the experiments which we discuss below, the influence of the (other than hydrostatic) pressure gradient and temperature gradient is assumed negligible, so that the particle flux can be written as an expansion in the concentration gradient in the form

$$\mathbf{J} = \mathbf{V}(c)c - D(c)\nabla c \ . \tag{1.2}$$

From the works by Batchelor the kinetic coefficients of dilute systems $\mathbf{V}(c)$ and $D(c)$ are known for small enough particles when the Brownian motion dominates [3–5]. These mixtures are called colloids and they are described by a structureless particle-particle correlation function. Batchelor's theory provides results for monodispersive and polydispersive suspensions. The case of larger particles which are fairly insensitive to the thermal noise corresponds to mixtures called suspensions. The particle-particle correlation function is determined by hydrodynamic interactions and remains unknown in this case, and consequently the value of the kinetic coefficient is unavailable theoretically. We avoid the unresolved issue by making a simple estimate of hydrodynamic diffusivity which uses the arguments originally discussed by Caflisch and Luke [6] and Hinch [7]. As for the velocity of hindered settling, it will be described by an empirical dependence.

Equations (1.1) and (1.2) with c dependences of different complexity have been considered by a number of authors. It was recognized [8,9] that Eqs. (1.1) and (1.2) with c-dependent velocity resemble very closely the famous Burgers equation of one-dimensional compressible flow [2,10]. This equation leads naturally to shock waves in which the nonlinear velocity dependence on concentration is balanced by diffusivity. Some nonlinear aspects of this effect were studied long ago by Kynch [11], who discussed the shock wave toppling in the absence of diffusivity, and more recently by Barker and Grimson [8] and by van Saarloos and Huse [9]. Baker and Grimson pointed out the fact that the Burgers equation has an analytical solution (if the concentration dependence of diffusivity is neglected) and argued its qualitative applicability to a sedimentation experiment [12]. The paper by van Saarloos and Huse [9] used the Burgers equation to discuss the sedimentation layers which are sometimes observed in the course of sedimentation.

Other versions of the continuity equations (1.1) and (1.2) have also been considered. Auzerais *et al.* [13] considered the effect of particle interaction and made comparison to experimental data for the case of vanishing diffusivity. Davis and Russel [14] and Nir and Acrivos [15] reported some analytical and numerical results for a particular version of kinetic coefficients; see also [16]. Comparison to experimental data in a more complex system with a steady shear flow of liquid was reported by

Schauflinger, Acrivos, and Zhang [17].

In the present paper we seek a quantitative comparison between the time-dependent evolution predicted by the Burgers equation and experimental data [18–20]. In the polydispersive case we introduce a system of coupled Burgers equations. Their solution describes the motion of the suspension interface proposed by Smith [21] and, in implicit form, by Davis and Acrivos [22]. The coupled Burgers equations predict an interesting phenomenon, which we termed *phase shifts;* it may already be observed in a bidispersive system. The particle size distribution function evolves in an interesting way near the interface. Step by step the system eliminates particles with different sizes. We call this evolution *renormalization* since it is produced by applying many times a given rule of eliminating the fastest species (infinitely many times in the continuum limit).

The paper is organized as follows. The Burgers equation is introduced in Sec. II and relevant kinetic coefficients are discussed. To show how this equation works, the experimental data of Ref. [19] for a colloid are compared with the analytical solution. In Sec. III we use coupled Burgers equations to describe polydispersive systems. We first address the unique steady-state motion in terms of simple analytical formulas borrowed from physics of the one-dimensional compressible gas [2] and then simulate the bidispersive case numerically to investigate the evolution of the initial condition problem. Description of the continuous polydispersive case is presented in Sec. IV. Then a comparison with experiments [18,20] is presented.

II. MONODISPERSIVE SEDIMENTATION

Depending on the particle size one distinguishes suspensions and colloids for a given fluid. The boundary is defined somewhat arbitrarily through a Péclet number,

$$\mathrm{Pe}=\frac{2aV_0}{D_0}=\frac{8\pi g\Delta\rho a^4}{3k_BT} , \tag{2.1}$$

which describes competition between the action of (say) gravity and thermal fluctuations on a spherical particle of radius a. Gravity results in particle downward motion with the Stokes velocity V_0,

$$V_0=\frac{(4/3)\pi a^3 g\Delta\rho}{6\pi\eta a}=\frac{2a^2 g\Delta\rho}{9\eta} , \tag{2.2}$$

due to the density difference $\Delta\rho$ in a fluid with viscosity η in the presence of gravity acceleration g. Thermal fluctuations are the source of the Brownian diffusivity

$$D_0=\frac{k_BT}{6\pi\eta a} , \tag{2.3}$$

where k_BT is the temperature in energy units. Systems with $\mathrm{Pe}<1$ are conventionally called colloids. For water at room temperature and particles less that 1 μm Brownian effects usually dominate, while larger particles form suspensions.

The concentration profile in the dilute limit $c(x,t)$ obeys a Burgers-like equation

$$\partial_t c=\partial_x[V(c)c]+\partial_x[D(c)\partial_x c] , \tag{2.4}$$

where $V(c)$ and $D(c)$ represent the Stokes velocity and gradient diffusivity modified by the presence of other particles. The axis x is directed upward, opposite to the direction of gravity. If $c(x,t)$ is normalized to be the volume fraction ($c=\frac{4}{3}\pi a^3 n$ with n being the number density), then

$$V(c)=V_0 f_v(c) , \tag{2.5}$$

where $f_v(c)$ is the hindering effect and

$$f_v(c)=1-kc+O(c^2),\quad c\ll 1 . \tag{2.6}$$

According to calculations by Batchelor [3], $k\approx 6.55$ in the dilute limit, $c\ll 1$. Larger values of the concentration are sometimes approximated, for example, by the Richardson-Zaki empirical formula [23], $f_v(c)=(1-c/c_0)^{kc_0}$ which works also in the case of suspensions. (There exist other suggested formulas [19].) Here $c_0<1$ is the volume fraction at dense packing.

The diffusivity D entering (2.4) can be written as

$$D_b(c)=D_0 f_b(c) , \tag{2.7}$$

with (again according to Batchelor [5]; see also [24])

$$f_b(c)=1-(k-8)c+\cdots\approx 1+1.45c,\quad c\ll 1 . \tag{2.8}$$

The nonlinear terms in the expansion (2.8) (studied experimentally [24]) lead to a maximum of f_b at $c\sim 0.15$, so that the entire concentration dependence of the diffusivity is within 10% of its bare values up to the volume fractions $c\sim 0.3$.

Addressing now suspensions, in the case of large Péclet numbers, we deal with strongly interacting systems, and the applicability of Eq. (2.4) is unclear. If assumed, it introduces a function $D(c)$ called hydrodynamic diffusivity [7]. This concept is an attempt to get the main effect of multiparticle forces without a very detailed calculation and can only be justified *a posteriori.*

Hinch [7] pointed out an argument by Caflisch that uniform distribution with finite particle sizes leads to convective flows due to density fluctuations. Hinch speculated that the convection will cease at a level of mixing which is comparable to the interparticle separation $ac^{-1/3}$. The velocity fluctuations of the "remaining" convection are then of the order of the main term of the interparticle force evaluated at the interparticle distance. This gives for the velocity fluctuation an estimate of $V_0c^{1/3}$. We may continue this speculation by multiplying these two values,

$$D_h(c)=k'aV_0,\quad c\ll 1 , \tag{2.9}$$

where k' is a pure number. Using (2.9) one finds that the ratio D_h/D_b is of the order of the Péclet number. If the dependence on concentration in Eq. (2.9) is incorrect, there will exist an additional class of mixtures which cannot be ascribed to either suspensions or colloids. The difference between vertical and horizontal fluctuations is not captured by the semiquantitative arguments above.

Equation (2.9) is in conflict with results by Koch and

Shaqfeh [25], based on an uncontrolled approximation. In the latter case the so-called "screening" length is of the order of ac^{-1}, and the velocity fluctuation is of order V_0. As a result the hydrodynamic diffusivity is aV_0/c and diverges in the dilute limit.

Experimentalists have been analyzing hydrodynamic diffusion by two different techniques. One approach [18,20] is to investigate the gradient diffusion. The other is to trace a marked particle and evaluate the self-diffusivity [26–29]. In a strongly interacting system the two approaches may, in principle, produce different values. Ham and Homsy [26] found that for the case of self-diffusion the factor k' depends upon concentration for small $c<0.01$, and saturates at about $k'=5$ for larger values of c. Experiments by Nicolai *et al.* [27,28] discriminate between vertical and horizontal self-diffusivities and may indicate that $k'=6-10$ for the former. Xue *et al.* [29] found a finite value of the velocity fluctuations in their dilute limit. This measurement supports the Koch-Shaqfeh result, and the viewpoint that hydrodynamic diffusivity diverges at small volume fractions [30].

We found $k'=10$ by analyzing the gradient diffusion of the experiments [18–20] (see Sec. IV). This estimate is within the error bars of the experimental estimates of self-diffusivity. The c dependence of D_h was not really tested in this paper since both the degree of polydispersity and uncertainty of the size distribution function used in [18–20] are found to be too large for this purpose.

Let us now use the Burgers equation to describe the results of experiments on monodisperse sedimentation. The Burgers equation with relevant boundary conditions $c(-\infty,t)=c_0>0$, $c(\infty,t)=0$ forms a solution which is called a single Burgers shock moving with constant speed and width. Substituting $c(x,t)=c(x+vt)$ into (2.4) and integrating from x to ∞ one obtains

$$D(c)\frac{dc}{dx}=[v-V(c)]c \ , \tag{2.10}$$

which for large negative x gives $v=V(c_0)$. The shape of the interface can be found by another integration of Eq. (2.10). This shape depends upon Péclet number [16]. At intermediate times the interface profile is time dependent. We found such a measurement in the paper by Al-Naafa and Selim [19]. The solution of Eq. (2.4) with initial condition $c(x,0)=c_0\theta(x)$ is

$$\begin{aligned} c(x,t)&=\frac{c_0 f_1(x,t)}{f_2(x,t)+f_1(x,t)} \ , \\ f_1(x,t)&=\exp\left\{-\frac{V_0 k c_0}{D_0}[x+V_0 t(1-kc_0)]\right\} \\ &\quad\times\left\{1-\operatorname{erf}\left[\frac{x+V_0 t(1-2kc_0)}{2\sqrt{D_0 t}}\right]\right\} , \\ f_2(x,t)&=1+\operatorname{erf}\left[\frac{x+V_0 t}{2\sqrt{D_0 t}}\right] . \end{aligned} \tag{2.11}$$

We then compare the data in Fig. 5 of Ref. [19] with this formula. The result is shown in Fig. 1. The experimental

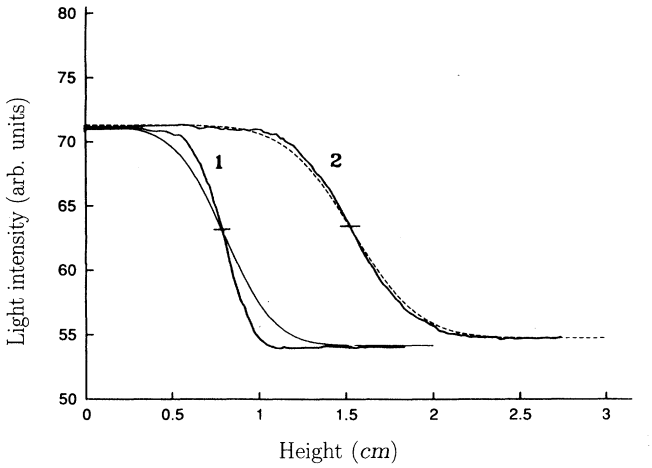

FIG. 1. Fit of light intensity data versus tube height for a monodispersive suspension [19]. Curve 1 was taken after 195.2 h after the beginning of experiment and curve 2 after 374.7 h. Experimental parameters used for the fit: $a=65$ nm, $c_0=0.009$, $\Delta\rho=1.005$ g cm^3, $V_0=0.12\times10^{-5}$ cm/sec. $T=25$ °C, so that $\eta=0.0077$ g/cm sec and $D_0=4.4\times10^{-8}$ cm^2/sec. Both curves are scaled in the vertical direction to meet the experimental range of Fig. 5 in Ref. [19]. This is the experiment at small Péclet numbers, so that hydrodynamic diffusivity is negligible with respect to the Brownian part.

parameters are given in the figure caption. Initially the shape of the optical density profile is narrower than the prediction of formula (2.11). After a transient we get an optical shape which does fit [31].

III. BIDISPERSIVE SEDIMENTATION

We then consider the case of bimodal distribution of particle sizes. Let c_1 and c_2 be the concentrations of these particles, both obeying continuity equations (1.1). The corresponding fluxes J_1 and J_2 are

$$J_i=V_i(c_1,c_2)-D_{ij}(c_1,c_2)\frac{\partial c_j}{\partial x} \ . \tag{3.1}$$

Using expansion at small concentrations we arrive at the two coupled Burgers equations

$$\begin{aligned} \partial_t c_1&=V_1\partial_x[(1-k_{11}c_1-k_{12}c_2)c_1]+D_1\partial_x^2 c_1 \ , \\ \partial_t c_2&=V_2\partial_x[(1-k_{21}c_1-k_{22}c_2)c_2]+D_2\partial_x^2 c_2 \ . \end{aligned} \tag{3.2}$$

This system is a straightforward generalization of the monodispersive Burgers equation (2.4). The hindering velocity of each of the particle species depends linearly on both volume fractions. This dependence has been studied by Batchelor and Wen; see Ref. [4] where one can find a method of computing the constants k_{11}, k_{12}, k_{21}, and k_{22}. The dependence of diffusivities D_1 and D_2 upon particle concentrations will be ignored in this section together with the cross terms when a gradient of, say, c_1 influences a flux of c_2 particles. These refinements vanish with c.

First, we are looking for steady-moving solutions

$c_{1,2}(x-v_{1,2}t)$. Substituting these into Eqs. (3.2) and integrating once we have

$$D_1\frac{dc_1}{dx}=(v_1-V_1)c_1+V_1k_{11}c_1^2-V_1k_{12}c_1c_2 \qquad (3.3)$$

and an analogous second equation. Two shocks may be observed for the relevant boundary conditions $c_{1,2}(-\infty)=c_{01,02}$, $c_{1,2}(\infty)=0$. We then have to decide which of the waves is faster. Without loss of generality let us assume that $v_1>v_2$ where

$$v_1=V_1(1-k_{11}c_{01}+k_{12}c_{02}) , \qquad (3.4)$$

$$v_2=V_2(1-k_{21}c_{01}+k_{22}c_{02}) . \qquad (3.5)$$

This leads to the first shock velocity being v_1. The substance 2 changes its concentration when the first shock passes through. Let us denote this changed (we shall also call it renormalized) concentration as c_2^*. At the top of substance 1 we essentially have the problem of monodispersive sedimentation considered in the previous section. Let the hindered velocity of settling be v_2^*; as we have seen above, it is also the velocity of the second shock. The concentration c_2^* obeys the quadratic continuity equation in the reference frame moving with the first shock velocity v_1 (see Ref. [2], Chap. IX, and Ref. [21]),

$$c_2(v_2-v_1)=c_2^*(v_2^*-v_1) . \qquad (3.6)$$

Here v_2^* is

$$v_2^*=V_2(1-k_{22}c_2^*) . \qquad (3.7)$$

Figure 2 illustrates the steady-state geometry of the system. It can be easily shown that if $v_1>v_2$ then $v_1>v_2^*$, and $v_1\to v_2^*$ when $v_1\to v_2$. Consequently, no other steady-moving solutions exist for this system. Thus, the steady-moving solution of coupled Burgers system is characterized by the formulas for the interface (shock) velocities. It is nice to get to know that these formulas also describe the solutions of coupled Burgers equations. Experimental confirmation of the shock velocities predicted by Eqs. (3.6) and (3.7) for bidispersive (and tridispersive) systems can be found in Refs. [24,32].

The coupled Burgers equations also allow one to study the transient regimes prior to the establishing of the steady-moving shocks. We hope to encourage studies of time-dependent phenomena by addressing the physics of coupled Burgers equations. To give an example of transient behavior we solved the system of two coupled Burgers equations numerically.

The two shocks when formed separate linearly in time and their asymptotic shapes may be found by numerical integration of Eq. (3.3) with real concentration dependences of the diffusivities; see [5]. Both shocks have finite widths (analytical formulas may be obtained in a number of limits) and quickly cease to interact; see Fig. 2. It must be emphasized that no matter how simple the steady-moving solution of the system (3.2) may seem, the transition to this solution in time may be rich; see Fig. 3 where a change in coupling constant k_{21} from 0.35 to 0.4 resulted in the system's inability to reach the dynamical steady state within the integration time. Figures 2 and 3 show examples of the time-dependent solutions of Eqs. (3.2) which develop transient increases of concentration and even additional transient shocks (Fig. 3). The final profiles in Fig. 2 display the two regions discussed above: the first shock at $x\approx 30$, accompanying renormalization of c_2 from 1 up to 1.86: and the second shock at $x\approx 45$ at the end of the integration time. Measuring the rate of change of the separation between adjacent profiles one can verify that the shock velocity is nicely predicted by Eqs. (3.4) and (3.7). However, the separation between the shocks accounts for the initial condition and interaction at the stage of shock "disentanglement" as well as for the widths of shocks.

The described behavior is yet another example of the dynamics of compressible one-dimensional gases [2].

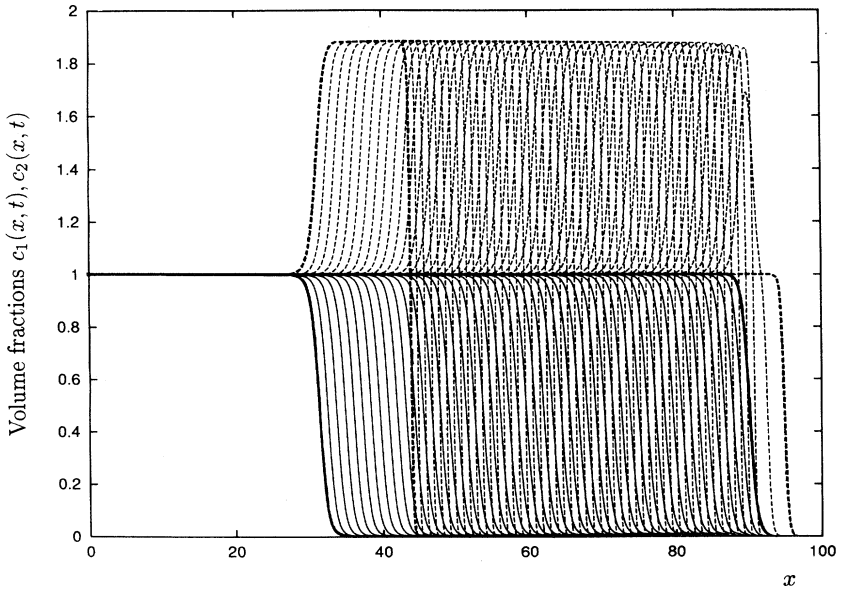

FIG. 2. Numerical integration of two coupled Burgers equations (3.2). Parameters: $V_1=0.1$, $V_2=0.05$, $k_{11}=k_{12}=k_{22}=0.4$, $k_{21}=0.35$, and $D_1=D_2=0.01$. Initial conditions for $c_1(x)$ and $c_2(x)$ were selected to be their individual Burgers shocks in the absence of coupling with small shift with respect to each other; $c_{-\infty}=1$, $c_{+\infty}=0$ for both substances. Integration time $t=2000$ and $\Delta t=40$ between profiles. c_1 is shown in lines; c_2 with broken lines. System size $x=100$. The sign of velocities was selected such that the shock motion occurs from right to left. Initial and final profiles are shown with thick lines. Equations (3.2) do not impose any constraints on amplitudes of $c_{1,2}$. We can formally use the nonphysical range $c_{1,2}>1$.

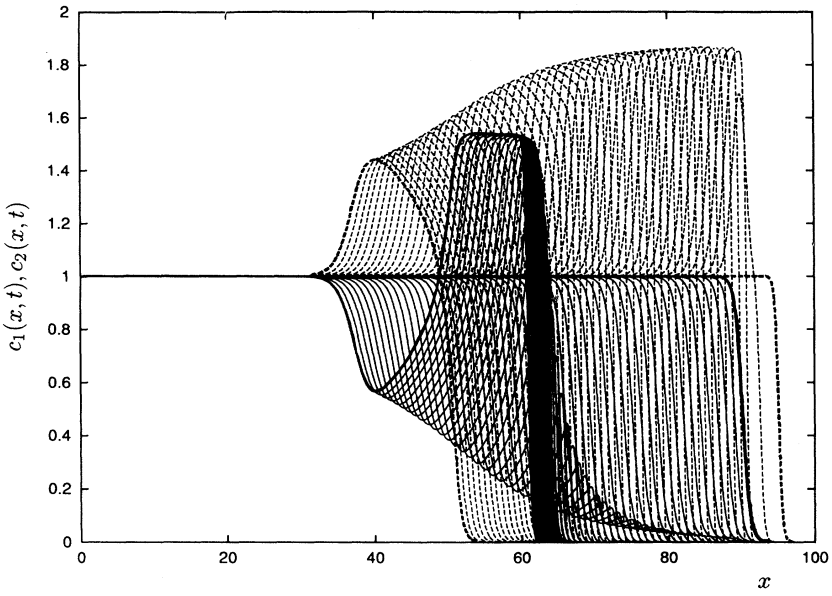

FIG. 3. An example of complex temporal behavior. Parameters are the same as in Fig. 2 except that $k_{21}=0.4$.

IV. POLYDISPERSIVE SEDIMENTATION

It is our intention to apply the ideas of the previous section to the real polydispersive case starting with the situation where a finite number N of particle sizes is involved and particle groups are numbered $1 \le i \le N$. As before one should calculate the hindered velocities of sedimentation of all particle groups which are given by

$$v_i = V_i \left[1 - \sum_{j=1}^{j=N} k_{ij} c_j \right] , \tag{4.1}$$

and represent a generalization of expressions like (3.4). Again we refer to Ref. [4] for the constants k_{ij}. The maximal velocity $\max_i(v_i)$ is to be found and the corresponding substance (say, i_0) will form the lowest (fastest) shock. Generally speaking, the motion of the edge of the size distribution is not necessarily the fastest; one may rather say that *some* substance i_0 will move down first, depending upon the matrix $k_{i,j}$ and the size (and density) distribution function. Other particle concentrations above the leader will be renormalized, according to the equations

$$v_i^* = V_i \left[1 - \sum_{j=1}^{j=N} k_{ij} c_j^* \right] , \tag{4.2}$$

$$c_i(v_i - v_{i_0}) = c_i^*(v_i^* - v_{i_0}) , \tag{4.3}$$

which form a system of quadratic equations. Note that the system can be formally extended to $i,j=i_0$ given that $c_{i_0}^*=0$.

Now the entire procedure is to be repeated N times. At each level of renormalization one additional substance is eliminated and others get renormalized. An example can be seen in Fig. 4 for the evolution of an initially Gaussian-like size distribution function with $N=26$ different particle sizes, and real parameters taken from [18]. In this particular case there is no inversion of ordering, i.e., larger sizes are eliminated first. The result of the calculation is a sequence of successively eliminated particle species and corresponding velocities. The interface shape becomes wider in time, although not as wide as one would obtain without renormalization. The concentration profile in the limit of vanishing diffusivity can be found by adding regions with renormalized concentrations at separations prescribed by successive velocity differences. Renormalization leads to thinner interfaces; this is the so-called phenomenon of *self-sharpening* of the interface [18,20] when smaller particles above larger particles move faster than they would do if mixed with larger particles. When diffusivity is finite, a contribution to the interface width comes from the phase shifts.

Before moving on to the continuous case we discuss the influence of diffusivity from a different perspective. For a single Burgers shock connecting concentration change

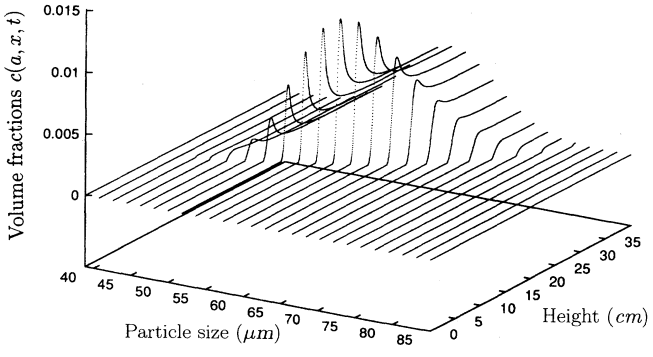

FIG. 4. Snapshot of the solution $c(a,x,t)$ at time $t=36$ min for the experiment [18]. Parameters: $a=61(\pm 6)$ μm, $\Delta\rho=1.384$ g/cm^3, $c_0=0.05$, and $\eta=0.0085$ g/cm sec. With these parameters one obtains $V_0(a)=0.0141$ cm/sec and $D_h(a)=k'\times 8.510^{-5}$ cm^2/sec. The value $k'=1$ is used (see Fig. 5). System length is 40 cm; an initially Gaussian size distribution with deviation 6 μm is used. Number of species $N=26$ and 1600 spatial points for each particle species.

from $c_{-\infty}$ to $c_{+\infty}$ the width is given by

$$W=\frac{2D}{V_0 k(c_{-\infty}-c_{+\infty})}\ , \tag{4.4}$$

where for a moment we assume the simplest possible situation: constant diffusivity and monodispersive case. The smaller is the concentration difference the weaker is the nonlinear effect competing with constant diffusivity [10], and the shock width becomes proportionally larger. A similar phenomenon exists in the polydispersive case; the larger is the number of different particle sizes which are taken into consideration, the smaller are the concentration changes and the smaller are the velocity differences. In addition, the widths of the successive shocks overlap. Thus, diffusivity provides a time-dependent cutoff for the achieved resolution in particle size step.

This physics is reflected in the renormalization of the size distribution function. When particles of a given size move down and are not present at some height, the distribution function of this size at that height becomes zero [rigorously speaking, it is, of course, of the order of exponentially small, $\exp(-Vx/D)$ diffusive corrections]. In the limit of large N this leads to a discontinuity which moves monotonically or jumps depending on the absence or presence of the ordering inversion discussed above. Discontinuous renormalization of the size distribution function implies that diffusivity is to be taken into account, and the existence of the diffusive time-dependent cutoff regularizes the problem. At any point along the interface new structure appears as time goes on. The minimal resolved size step diminishes with time, and the emerging of the fine structure of the distribution function (or segregation) continues. Note that certain integrated properties such as the profile of the optical density may still be perfectly smooth under these circumstances; it is the size distribution function which changes most drastically within the suspension interface.

In the continuous case the coupled Burgers equations form an integro-differential equation for the evolution of the size distribution function $c(a,x,t)$:

$$\frac{\partial c(a,x,t)}{\partial t}=V_0(a)\frac{\partial}{\partial x}\left[c(a,x,t)-\int_0^\infty da' k(a,a')c(a,x,t)c(a',x,t)\right]+\frac{\partial}{\partial x}\int_0^\infty da' D(a,a')\frac{\partial c(a',x,t)}{\partial x}\ , \tag{4.5}$$

where the kernel $k(a,a')$ is the continuous generalization of the matrix k_{ij} and the diffusivity is a functional of c with diagonal terms of zero and first order in c and off-diagonal terms of first order in c. The solution of Eq. (4.5) is well defined due to the presence of D. It is noteworthy that for the kernels $k(a,a')$ and $D(a,a')$, whose dependence on a and a' consists of factorizable terms, it may be more convenient to work with the Mellin transform of Eq. (4.5) performed in variable a.

Generalization of Eqs. (4.2) and (4.3) to the continuous case is straightforward. We consider the simplest case of no ordering inversion. Then at any point x on the interface (at late times) there exists maximal particle size $b(x)$ which is "eliminated" at this point. It is convenient to parametrize the spatial dependence by $b(x)$. Then concentration becomes a function of a and b, i.e., $c(a,b)$ [and certainly an implicit function of x through $b(x)$]. Particle hindered velocities are given by

$$\begin{aligned} v(a,b)&=V_0(a)\gamma(a,b)\ ,\\ \gamma(a,b)&=1-\int_0^b da' k(a,a')c(a')\ , \end{aligned} \tag{4.6}$$

and the continuity equation reads

$$c(a,b)[v(a,b)-v(b,b)]=c(a,b-db)[v(a,b-db)-v(b,b)]\ , \tag{4.7}$$

where

$$v(a,b-db)=V_0(a)\left\{1-\int_0^{b-db} da' k(a,a')c(a,b-db)\right\}\ . \tag{4.8}$$

Expansion of (4.6)–(4.8) to the first order to get an equation for $\partial c(a,b)/\partial b$ should be done carefully since $c(a,b)$ contains a singularity at $a=b$,

$$c(a,b)=\frac{C(b)}{(b-a)^{\mu(b)}}+c^R(a,b)\ , \tag{4.9}$$

where μ is positive, such that integral (4.6) converges, and $c^R(a,b)$ stands for the regular part at $a=b$. The exponent $\mu(b)$ can be related to other functions by using Eqs. (4.7) and (4.8). A study not presented here shows that

$$\mu(b)=\left.\frac{\partial \ln\gamma(a,b)/\partial b}{2/b+[\partial \ln\gamma(a,b)/\partial a]}\right|_{a=b}\ , \tag{4.10}$$

i.e., the concentration $c(a,b)$ becomes infinite at the point $a=b$. Given that the singularity is identified, explicit differential equations of renormalization can be written for dC/db and $\partial c^R(a,b)/\partial b$.

Numerical integration of Eq. (4.5) enables one to study the time-dependent evolution of polydispersive suspensions. For this purpose we performed simulations on a workstation to fit the experimental data by Davis and Hassen [18] and Lee *et al.* [20]. The simplest possible explicit difference scheme (Euler scheme) already works nicely for Eq. (4.5), provided that spatial and temporal steps obey the conditions $\Delta x \ll D/V_0$, $\Delta t \ll \min(\Delta x/V_0, \Delta x^2/D)$. The results cease to depend on numerical resolution for $N>30$ particles species (to model the size distribution function) and more than 1000 spatial points for each of the species given that the characteristic value of the hydrodynamic diffusivity exceeds 10^{-4} cm^2/sec. The diffusivity of particles of size a was selected to be $D_h=k'a_0V_0(a_0)$, where a_0 is the

average size. The results are presented in Figs. 4–6. Figure 4 shows the evolution of the size distribution function c and resembles closely the numerical results by Davis and Hassen (see their Fig. 2) if the latter are resolved in space. One can clearly see the appearance of singularities of the size distribution function. Their amplitude is restricted by diffusive resolution as we discussed above. Figure 5 compares the simulation results with the experimental data for transmitted light intensity, which is given by [18]

$$\ln[I(x,t)] \propto -\int \frac{da}{a} c(a,x,t) , \tag{4.11}$$

scaled to the experimental amplitude range $I(x,0)/I(x,\infty)=0.12$. The factor k' was the adjustable parameter. It is interesting to note that we did not find any significant dependence upon the constant k' for values of k' up to about 10. Also important is the observation that the interface width obtained at smaller k' (we tried $1 \leq k' \leq 10$) is nicely comparable to the experimentally measured one. Smaller values of k' require higher resolution or more advanced numerical schemes and were not attempted.

Thus it is possible to comment on the conclusion made by Davis and Hassen who used Eqs. (4.2) and (4.3) and discovered that in addition to the polydispersive width there is a diffusivelike contribution which they identified with the effect of gradient hydrodynamic diffusivity. However, the "bare" hydrodynamic diffusivity that

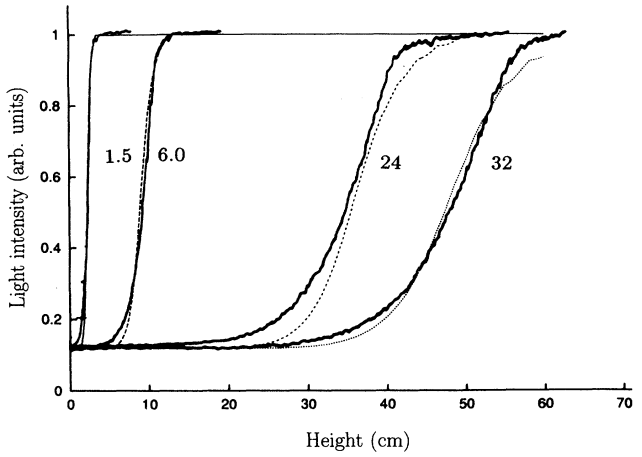

FIG. 5. Fit of raw transmitted light intensity versus time for a polydispersive suspension (Fig. 11 of Ref. [18]). The intensity is measured at heights $x=1.5$, 6.0, 24, and 32 cm. Note that we use $k=2.5$; this is the experimental value which can be extracted from Fig. 11 in contradiction with Table I (both from Ref. [18]). The other possible explanation is that Fig. 11 was, in fact, taken for $c_0=0.02$; then $k \sim 5$ in agreement with Fig. 12 of Ref. [18] and Table I. (In both cases the conclusion made in the text remains valid.) The Richardson-Zaki dependence $(1-c)^k$ is employed instead of $1-kc$; here c is the total volume fraction. The value $k'=1$ is used to show that the hydrodynamic diffusivity is not required to account for the width of the curves. At the top of the theoretical curves one can notice small oscillations caused by insufficiently large number of particle species $N=26$ when they get separated.

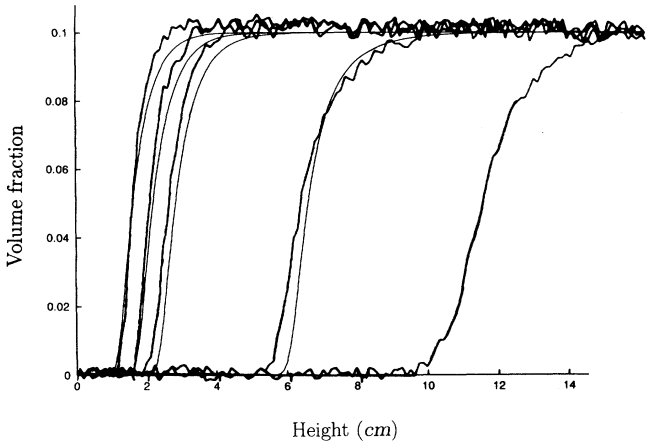

FIG. 6. Fit of volume fraction $\int da\, c(a,x,t)$ vs height x for four different times: 332, 443, 567, and 1288 sec from left to right. Last experimental curve at 2611 sec is not fitted since its average displacement is not described by a motion with constant velocity (see text). Experimental curves are from Fig. 2 of Ref. [20]. Parameters: $a=67.9(\pm 4.0)$ μm, $\Delta\rho=1.57$ g/cm^3, $\eta=0.0164$ g/cm sec, and $c_0=0.1$. With these parameters, $V_0=0.0096$ cm/sec and $D_h=k'\times 6.510^{-5}$ cm^2/sec. The value $k'=10$ is used. The Richardson-Zaki dependence $(1-c)^k$ is employed with c being the total volume fraction here.

enters Eqs. (2.4) and (4.5) does not contribute to the interface width directly—it is achieved through the evolution of the equation, and the distribution of the phase shifts influences the width. The simulation of the coupled Burgers equation (4.5) becomes a necessary step to describe the results of the polydispersive sedimentation experiment. It should also be noted that the tail of the interface profile is sensitive to the real particle size distribution (which is not necessarily Gaussian as assumed in Fig. 5 and in Ref. [18]).

An analogous fit was performed for the data in Fig. 2 of Ref. [20]. The fit is shown in Fig. 6. Here the experimental standard deviation of particle size was only $\frac{2}{3}$ of that of Ref. [20], and polydispersity alone cannot account for the observed width. With the help of hydrodynamic diffusivity (using $k'=10$) we can get curves which are rather similar to the experimental ones. The exception is the last curve, whose position is not described by motion with a constant velocity. We are thankful to Soonchil Lee who explained to us that the shape and position of this curve is affected by the presence of the lower interface between the suspension and sediment, and must be ignored in our analysis [33].

V. CONCLUSION

Application of (coupled) Burgers equations to describe sedimentation of (polydispersive) suspensions and colloids enables one to reproduce experimental data and provides a basis for analyzing time-dependent sedimentation. The study of the fluctuations of concentration during sedimentation may lead to an experimental realization of Burgers turbulence.

ACKNOWLEDGMENTS

I am grateful to David Grier, Daniel Mueth, John Crocker, and Elisabeth Guazzelli for discussions, and to Leo Kadanoff for his constant interest and help with the manuscript. Numerical simulations of the two coupled Burgers equations were made by Michael Brenner; his participation is gratefully acknowledged. The work was supported in part by the MRSEC Program of the National Science Foundation under Grant No. DMR-9400379 and in part by NSF Grant No. NSF-DMR-90-15791.

[1] Y. Zimmels, Powder Technol. **70**, 109 (1992).
[2] L. D. Landau and E. M. Lifshitz, *Fluid Mechanics* (Pergamon, New York, 1975).
[3] G. K. Batchelor, J. Fluid Mech. **52**, 245 (1972).
[4] G. K. Batchelor, J. Fluid Mech. **119**, 379 (1982); G. K. Batchelor and C.-S. Wen, *ibid.* **124**, 495 (1982); J. M. Revay and J. J. L. Higdon, *ibid.* **243**, 15 (1992).
[5] G. K. Batchelor, J. Fluid Mech. **74**, 1 (1976).
[6] R. E. Caflisch and J. H. C. Luke, Phys. Fluids **28**, 759 (1985).
[7] E. J. Hinch, in *Disorder and Mixing,* edited by E. Guyon, J.-P. Nadal, and Y. Pomeau, NATO Advanced Study Institute, Series E: Applied Sciences, Vol. 152 (Kluwer, Dordrecht, 1988).
[8] G. O. Barker and M. J. Grimson, J. Phys. A **20**, 305 (1987).
[9] W. van Saarloos and D. Huse, Europhys. Lett. **11**, 107 (1990).
[10] The basic references on Burgers equations are J. M. Burgers, *The Nonlinear Diffusion Equation* (Reidel, Dordrecht, 1974); G. B. Witham, *Linear and Nonlinear Waves* (Wiley, New York, 1974).
[11] G. J. Kynch, Trans. Faraday Soc. **48**, 166 (1952).
[12] M.-C. Anselmet, R. Anthore, X. Auvray, C. Petipas, and R. Blanc, C. R. Acad. Sci. Ser. II **300**, 69 (1985).
[13] F. M. Auzerais, R. Jackson, W. B. Russel, and W. F. Murphy, J. Fluid Mech. **195**, 437 (1988); **221**, 613 (1990).
[14] K. E. Davis and W. B. Russel, Phys. Fluids A **1**, 82 (1989).
[15] A. Nir and A. Acrivos, J. Fluid Mech. **212**, 139 (1990).
[16] W. B. Russel, D. A. Seville, and W. R. Scholwalter, *Colloidal Dispersions* (Cambridge University Press, Cambridge, England, 1989).
[17] U. Schauflinger, A. Acrivos, and K. Zhang, Int. J. Multiphase Flow **16**, 567 (1990).
[18] R. H. Davis and M. A. Hassen, J. Fluid Mech. **196**, 107 (1988).
[19] M. A. Al-Naafa and M. S. Selim, AIChE J. **38**, 1618 (1992).
[20] S. Lee, Y. Jang, C. Choi, and T. Lee, Phys. Fluids A **4**, 2601 (1992).
[21] T. N. Smith, Trans. Inst. Chem. Eng. **44**, 153 (1966).
[22] R. H. Davis and A. Acrivos, Annu. Rev. Fluid Mech. **17**, 91 (1985).
[23] J. F. Richardson and W. N. Zaki, Trans. Inst. Chem. Eng. **32**, 35 (1954).
[24] M. A. Al-Naafa and M. S. Selim, Fluid Phase Equilibria **88**, 227 (1993).
[25] D. L. Koch and E. S. G. Shaqfeh, J. Fluid Mech. **224**, 275 (1991).
[26] J. M. Ham and G. M. Homsy, Int. J. Multiphase Flow **14**, 533 (1988).
[27] H. Nicolai, B. Herzhaft, L. Oger, E. Guazzelli, and E. J. Hinch, Phys. Fluids **7**, 12 (1995).
[28] H. Nicolai and E. Guazzelli, Phys. Fluids **7**, 3 (1995).
[29] J.-Z. Xue, E. Herbolzheimer, M. A. Rutgers, W. B. Russel, and P. M. Chaikin, Phys. Rev. Lett. **69**, 1715 (1993).
[30] I am grateful to Paul Chaikin for a clarifying discussion on this subject.
[31] Our attempt to use a more complex fit (see Sec. IV for the description of the polydispersive fit) by taking into account the small polydispersity of the suspension (± 4.5 nm) did not result in significant changes. If the transient is real one needs more experimental data to help resolve this issue.
[32] R. H. Davis and K. H. Birdsell, AIChE J. **34**, 123 (1988).
[33] Soonchil Lee (private communication).